Materials Transactions, Vol. 49, No. 1 (2008) pp. 2 to 6
Special Issue on Severe Plastic Deformation for Production of Ultrafine Structures and Unusual Mechanical Properties: Investigating Role of High-Density Lattice Defects

Evolution of Microstructure and Hardness in Pure Al by Twist Extrusion

Dmitry Orlov[1], Yan Beygelzimer[1], Sergey Synkov[1], Viktor Varyukhin[1] and Zenji Horita[2]

[1]*Donetsk Institute for Physics & Engineering of the National Academy of Sciences of Ukraine, 72 R. Luxembourg St., Donetsk, 83114, Ukraine*
[2]*Department of Materials Science and Engineering, Faculty of Engineering, Kyushu University, Fukuoka 819-0395, Japan*

High purity Al (99.99%) is subjected to severe plastic deformation (SPD) at room temperature using a process of twist extrusion (TE). The microstructure evolution and the related change in microhardness are examined with respect to imposed strain. It is shown that subgrains develop after the first TE pass with a size of ~1.6 μm and this size remains essentially the same for further application of TE passes. However, dislocations become less visible within grains and grain boundaries become straight and well-defined with misorientation angle higher as the imposed strain is increased. The hardness increases with imposed strain when the magnitude of the strain is small. However, as the imposed strain is large, the hardness decreases due to a reduction of dislocations within grains. It is confirmed that these results obtained with TE are consistent with those reported using equal-channel angular pressing (ECAP) and high pressure torsion (HPT), indicating that the microstructural change and the variation of related mechanical properties with straining observed in pure Al are not affected significantly by the methods of SPD processing. [doi:10.2320/matertrans.ME200724]

(Received September 5, 2007; Accepted October 23, 2007; Published December 12, 2007)

Keywords: *aluminum, twist extrusion, severe plastic deformation, hardness, transmission electron microscopy*

1. Introduction

Severe plastic deformation (SPD) is well-proved technology for production of bulk ultrafine- and nano-grained structures in metallic materials.[1–3] Among many processing techniques available for SPD, twist extrusion (TE) is known as a promising SPD process.[3–6] However, TE has been less studied[7] and little is known for the evolution of microstructure and mechanical properties during TE process. Therefore, this study is initiated in order to conduct TE using pure Al. The microstructures and mechanical properties are examined with respect to imposed strain. Pure Al is chosen for this study because the results of pure Al were well documented for other SPD processes such as equal-channel angular pressing (ECAP)[8–10] and high pressure torsion (HPT).[11]

2. Experimental

The experiments were conducted on 99.99% purity aluminum produced by ingot casting. Edge parts and 2 mm surface layers of the as-received ingot were machined out. Then the ingots were hydroextruded or cold rolled at room temperature (RT) into billets for TE with the cross-section of $18 \times 28\,\text{mm}^2$ as illustrated in Fig. 1(a) and cut to lengths of 100 mm. All the billets were annealed at 773 K for 1 hour and cooled in furnace. TE was conducted at RT using a tool set as shown in Fig. 1. The twisting die has a twist line slope with an angle of $\beta = 60^\circ$ in the counter clockwise direction. With this geometry, average true strain of ~1.2[4,5] is introduced for a single pass. As illustrated in Fig. 1(a), a billet was inserted into an entrance hole and pressed through the twisting channel using a plunger. The billet was not only pushed into the twisting channel but also to filled up the entrance hole as illustrated in Fig. 1(b). A backpressure of ~200 MPa was applied to the billets. The extrusion was performed at a speed ~3 mms^{-1}. This TE process was repeated up to 4 passes which come to a total average strain of ~4.8. This level of strain was selected because an UFG structure was attained by ECAP[8–10] and HPT.[11] As shown in Fig. 1(b), the three orthogonal directions of the billets were defined such that the extrusion direction (ED) is parallel to the longitudinal axis of the billet; the normal direction (ND) and the transverse direction (TD) are, respectively, parallel to the short and long axes on the cross-sectional plane perpendicular to the ED of the billet.

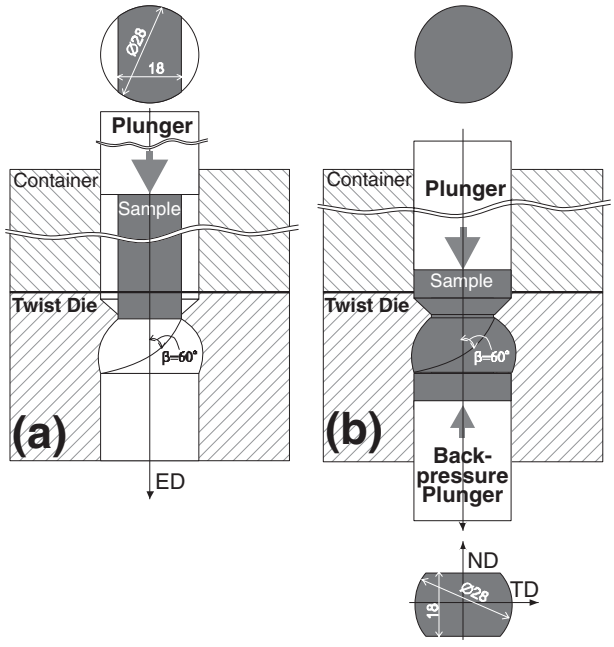

Fig. 1 Schematic illustration of twist extrusion (TE) used in this study: a) before TE processing and b) during TE processing.

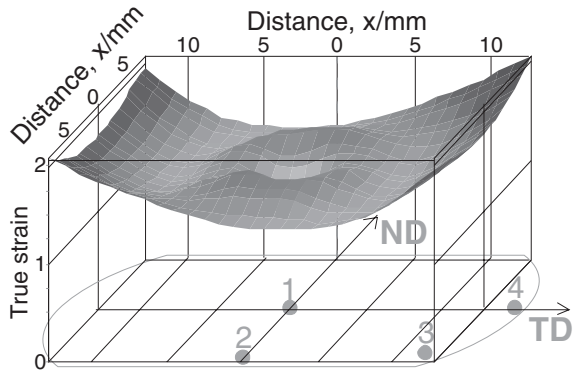

Fig. 2 Representative locations for TEM observation and magnitude of strain created through single pass of TE shown in cross-section perpendicular to ED direction.

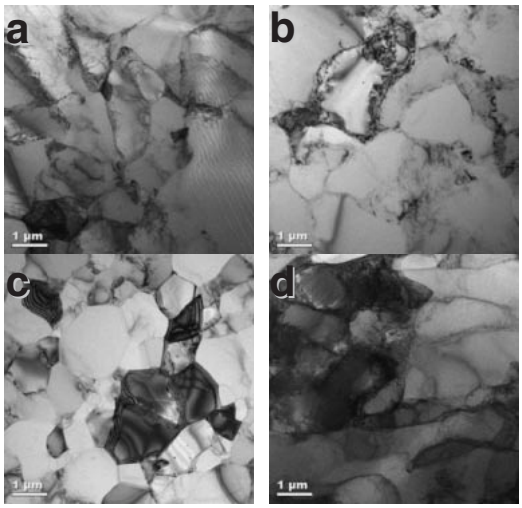

Fig. 3 TEM micrographs after 1 TE pass at locations of (a) position 1, (b) position 2, (c) position 3 and (d) position 4 marked in Fig. 2.

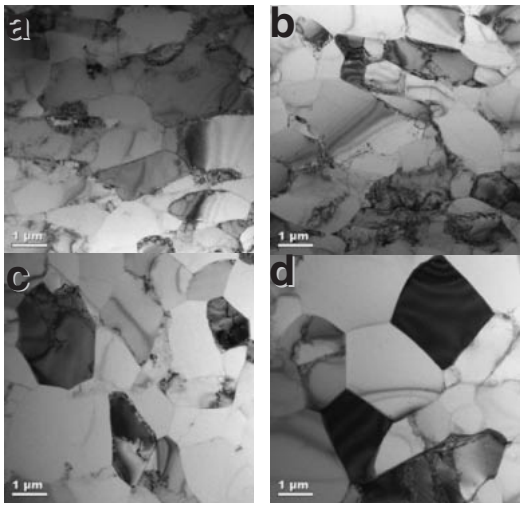

Fig. 4 TEM micrographs after 4 TE passes at locations of (a) position 1, (b) position 2, (c) position 3 and (d) position 4 marked in Fig. 2.

Microstructural observation of the TE-processed samples was conducted using transmission electron microscopy (TEM). In order to prepare thin samples for the TEM, rods of ~3 mm in diameter were cut by an electric discharge machine and they were sliced to disks with thicknesses of ~0.5 mm by an abrasive saw and mechanically ground by abrasive papers to final thicknesses of 0.13–0.15 mm. Such disks were electro-polished for perforation using twin-jet technique at RT in a perchloric-based solution. TEM observations were undertaken using a Philips Tecnai-20 transmission electron microscope operating at an accelerating voltage of 200 kV.

Electron backscatter diffraction (EBSD) analysis was also conducted using Hitachi S-4300SE equipped with a field emission gun at an accelerating voltage of up to 30 kV. Determination of crystal orientation involved automatic beam scanning with step sizes of 0.08–0.3 μm. Grain sizes and misorientation angles were determined along with the EBSD analysis. Data acquisition and subsequent analysis were performed using a TSL orientation image microscopy software (v.3.5). A cleaning-up procedure was applied to all EBSD images to adjust points with confidence index (CI) lower than 0.1. Misorientations less than 2° were excluded from the analysis because of the limitations of the angular resolution of the EBSD technique.[12)]

Vickers hardness (HV) tests were conducted using an Akashi MVK-E3 testing machine with an applied load of 25 g for 15 seconds. Specimens were cut in longitudinal and transversal directions by an abrasive saw, mechanically ground by abrasive papers and polished with a cloth containing suspension of silica powders. Hardness measurements were made with an interval of 0.5 mm to avoid any effect of neighboring indentations.

3. Results and Discussion

TEM observations were conducted at the representative areas on the cross-sections of the TE-processed billets as marked in Fig. 2. Figure 2 also shows a variation of strain throughout the cross section of the billet reproduced from a numerical analysis by Berta *et al.*[7)] The total equivalent strain introduced is increased as in the order of positions 1, 2, 3 and 4. TEM micrographs after 1 TE pass and 4 TE passes are shown in Fig. 3 and Fig. 4, respectively, where (a), (b), (c) and (d) correspond to micrographs at positions1, 2, 3 and 4 in Fig. 2, respectively. It appears that grains have almost a similar size of ~1.6 μm irrespective of the TE passes and the positions. However, when comparison is made between the samples after 1 pass and 4 passes but at the same position, there are less dislocations within grains after 4 passes than after 1 pass. Furthermore, while the grain boundaries appear to have some widths containing agglomeration of tangled dislocations after 1 pass, they are sharp and clear without any width after 4 passes. This difference is more prominent as the observation is made at positions 1 through 4, namely as the imposed strain is increased. It is concluded that dislocations are less visible within grains and grain boundaries become straight and well-defined as the imposed strain is increased. This trend is the same as observed after application of other

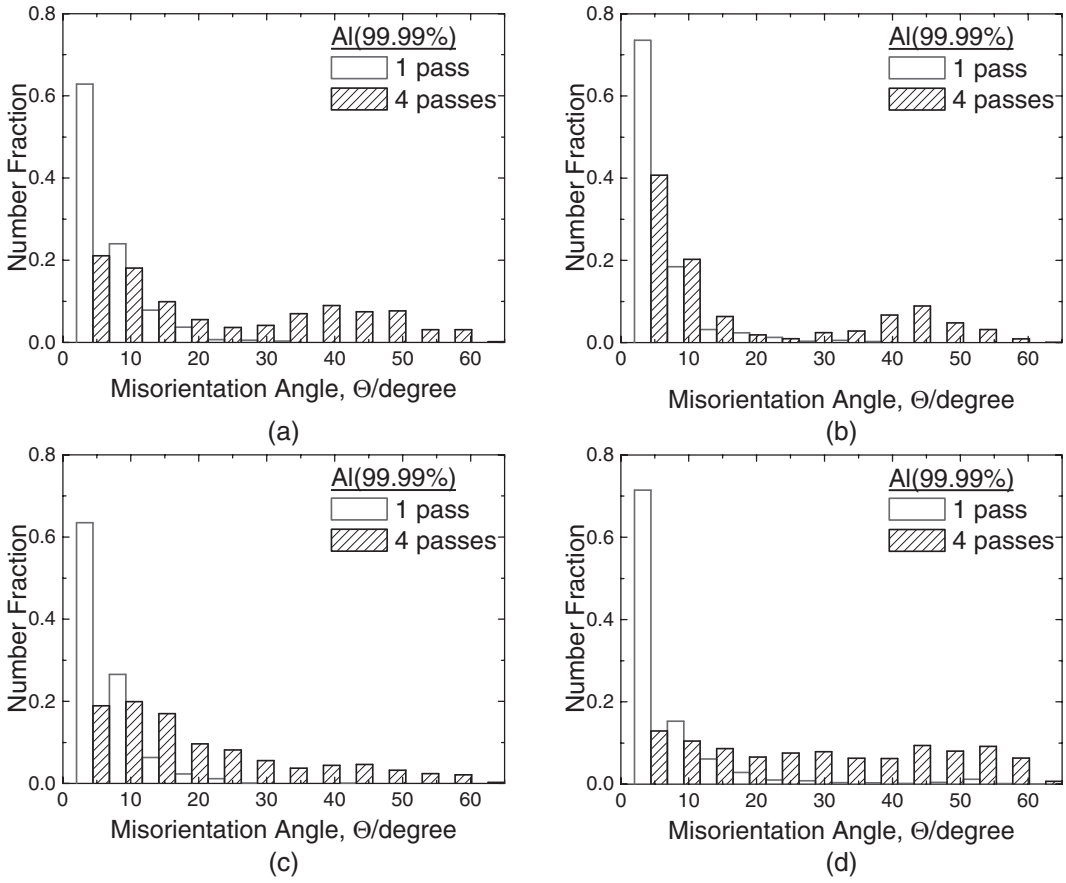

Fig. 5 Fraction of misorientation angle after 1 and 4 TE passes at locations of (a) position 1, (b) position 2, (c) position 3 and (d) position 4 marked in Fig. 2.

SPD processes such as ECAP and HPT.[8–11] Therefore, it turns out that the microstructural evolution with straining observed in pure Al is not affected significantly by SPD processing methods.

The change in misorientation angle with respect to the position and the number of TE pass is shown in Fig. 5 for both samples after 1 and 4 passes, where (a), (b), (c) and (d) are at positions 1, 2, 3 and 4, respectively. Low angle boundaries (LAB) are dominant after 1 pass but their fractions decrease significantly after 4 passes. Instead, more fractions of high angle boundaries (HAB) are generated after 4 passes. There is a slight increase in the fraction of HAB with position 1 to position 4 for both samples after 1 and 4 passes: for example, the fraction of HAB increases from 8% at position 1 to 15% at position 4 for the sample after 1 pass and from 53% at position 1 to 71% at position 4 for the sample after 4 passes.

Figure 6 shows variations of Vickers microhardness for samples after 1 pass and 4 passes, where (a) is the results measured along the diagonal line on the cross-section perpendicular to the ED (hereafter called the transverse section) and (b) is the results measured along the lines parallel to the ED at the center and edge parts on the cross-section perpendicular to the ND (hereafter called the longitudinal section). The measured locations are depicted in the inset in Fig. 6. For comparison, hardness variations after annealing but before TE are also included in Fig. 6. It is apparent that there is no anisotropy in the hardness of the annealed state before TE.

As shown in Fig. 6(a), there is a significant increase in hardness after TE when compared with the hardness in the annealed state before TE. The increasing behavior is different: in the center parts where the strain is less created, the hardness is higher for the sample after 4 TE passes than after 1 TE pass, while in the edge parts where large strain is created, the trend is opposite so that the hardness is lower for the 4 TE passes than 1 TE pass. These hardness variations are consistent with the reports of ECAP and HPT conducted on the 99.99%Al.[8–11] For ECAP, the hardness reaches a maximum after 2 ECAP passes and thereafter decreases with further numbers of pressings.[10] For HPT, the hardness is higher at the center of HPT disk and lower at the edge where the strain is introduced in proportion to the distance from the center and this hardness variation along the diameter of the disk disappears with the number of HPT revolutions to converge to the same level as the outer edge regardless of HPT revolutions and locations from the center of the disk.[11] It should be noted that the scattering of data points appears to be large after TE when compared with the scattering before TE. This suggests that there should be microstructural inhomogeneity developed through TE process on the cross-section perpendicular to the ED.

The hardness variations on the longitudinal section are shown in Fig. 6(b). It is apparent that the hardness level is

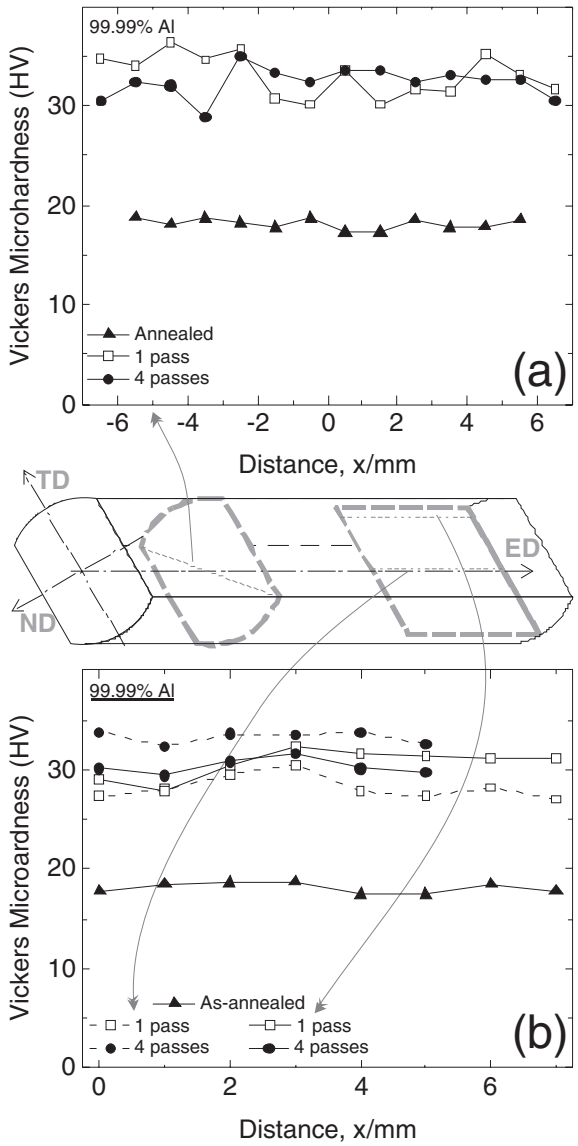

Fig. 6 Vickers microhardness measured along (a) diagonal line on cross-section as depicted in inset and (b) longitudinal lines at center and edge parts on longitudinal section as depicted in inset.

highest for the measurements along the central line of the sample after 4 TE passes and lowest along the central line after 1 pass. Between the two are the hardness levels along the lines at the edge part of the sample after 1 and 4 passes. This trend is again consistent with the hardness change observed with respect to the number of ECAP passes.[10] As shown in Fig. 2, the strain introduced is lowest at the center and is higher as the location is outward to the edge. The lowest hardness after 1 pass at the center indicates that dislocations are being accumulated but the accumulation is insufficient to maintain a higher level of hardness. As the number of TE passes, the dislocation density at the center increases to reach the highest level of hardness. The large strain is created at the edge part but the strain is now large enough for dislocations to disappear by mutual annihilation and rearrangement within grains. The same occurs after 4 passes but dislocations may be absorbed in the grain boundaries to be sharpened and well defined as shown in Fig. 4(d). It appears that these hardness measurements well correspond to the microstructural difference shown in Fig. 3 and Fig. 4.

As a final remark to this study, there are two important processes of structure evolution in 99.99%Al under TE operation: first, generation of dislocations and subsequent development of the deformation-induced low-angle grain boundaries, and second, a continuous reduction of dislocations and appearance of well-defined grain boundaries. When the imposed strain is small, the first process dominates, leading to an increase in the hardness level due to an increasing numbers of dislocations. When the imposed strain is large, the second process prevails over the first process and the hardness decreases due to a reduction of dislocations. Although the grain boundary increases in the misorientation angle, it does not much help an increase in hardness because the grain boundary itself acts as a dislocation absorber.

4. Conclusions

(1) Subgrains developed after the first TE pass with a size of $\sim$1.6 μm and this size remains essentially the same for further application of TE passes.
(2) Dislocations are less visible within grains and grain boundaries become straight and well-defined with misorientation angle higher as the imposed strain is increased.
(3) The hardness increases with an imposed strain when the magnitude of the strain is small. With an increasing application of imposed strain, the hardness decreases due to a reduction of dislocations within grains.
(4) The present results obtained with TE are consistent with those reported using equal-channel angular pressing (ECAP) and high pressure torsion (HPT) although their straining processes are different.
(5) The microstructural change and the related hardness variation with straining observed in pure Al are a common consequence after application of SPD processes.

Acknowledgements

This work was supported in part by the Light Metals Educational Foundation of Japan, in part by 21st COE program “Functional Innovation of Molecular Informatics” from the Ministry of Education, Culture, Sports, Science and Technology, Japan, and in part by a Grant-in-Aid for Scientific Research on Priority Areas “Giant Straining Process for Advanced Materials Containing Ultra-High Density Lattice Defects” from the Ministry of Education, Culture, Sports, Science and Technology, Japan.

REFERENCES

1) R. Z. Valiev, R. K. Islamgaliev and I. V. Alexandrov: Progress in Materials Science. **45** (2000) 103–184.
2) R. Z. Valiev and T. G. Langdon: Progress in Materials Science. **51** (2006) 881–981.
3) R. Z. Valiev, Y. Estrin, Z. Horita, T. G. Langdon, M. J. Zehetbauer and Y. T. Zhu: The Journal of Materials. **58** (2006) 33–39.

4) Y. Beygelzimer, D. Orlov and V. Varyukhin: *A New Severe Plastic Deformation Method: Twist Extrusion*. ed. by T. G. L. Y. T. Zhu, R. S. Mishra, S. L. Semiatin, M. J. Saran and T. C. Lowe., 2002 TMS Annual Meeting and Exhibition. Seattle, Washington, USA: TMS (The Minerals, Metals & Materials Society, 2002) p. 297–304.
5) Y. Beygelzimer, D. Orlov, A. Korshunov, S. Synkov, V. Varyukhin, I. Vedernikova, A. Reshetov, A. Synkov, L. Polyakov and I. Korotchenkova: Solid State Phenomena. **114** (2006) 69–78.
6) Y. Y. Beygelzimer, V. N. Varyukhin, S. G. Synkov, A. N. Sapronov and V. G. Synkov: Physics and Technology of High Pressures. **9** (1999) 109–110.
7) M. Berta, D. Orlov and P. Prangnell: Int. J. Mat. Res. **98** (2007) 200–204.
8) Y. Iwahashi, Z. Horita, M. Nemoto and T. G. Langdon: Acta Materialia. **46** (1998) 3317–3331.
9) S. D. Terhune, D. L. Swisher, K. Oh-ishi, Z. Horita, T. G. Langdon and T. R. McNelley: Metall. Mater. Trans. A. **33** (2002) 2173–2184.
10) Z. Horita, K. Kishikawa, K. Kimura, K. Tatsumi and T. G. Langdon: Mater. Sci. Forum, **558–559** (2007) 1273–1278.
11) C. Xu, Z. Horita and T. G. Langdon: Acta Mater. **55** (2007) 203–212.
12) F. J. Humphreys: Scripta Mater. **51** (2004) 771–776.